



## Research Paper

**Cite this article:** Wegner TE, Gebhardt S, Del Galdo G (2023). Fill level measurement of low-permittivity material using an M-sequence UWB radar. *International Journal of Microwave and Wireless Technologies* **15**, 1299–1307. <https://doi.org/10.1017/S1759078723000739>

Received: 06 December 2022  
Revised: 25 May 2023  
Accepted: 28 May 2023

### Keywords:

background subtraction; empty state estimation; level measurement; ultra wideband radar

**Corresponding author:** Tim Erich Wegner;  
Email: [tim-erich.wegner@tu-ilmenau.de](mailto:tim-erich.wegner@tu-ilmenau.de)

## Abstract

Due to increasingly complex and automated manufacturing processes, the demands on the control parameters of these processes are also increasing. One parameter is the fill quantity of, e.g., liquids in production plants, whose precise determination is of ever-growing importance. Up to now, the exact level of determination under difficult conditions, such as high ambient temperatures, has been a particular challenge. This paper demonstrates a novel method by which an M-sequence UWB radar can determine levels of low-permittivity materials in small metal containers. For this purpose, hot melt is used as an example. Thus, the influence of large temperature differences on the long-term stability of level measurement can also be investigated. The measurements show that the level of hot melt can be measured to be long-term stable with an accuracy of better than 3 mm. Furthermore, the precise determination of the empty state is highly important for many applications. For this reason, this paper shows a method for determining the empty state without complex calibration procedures. For the empty level indication, an accuracy of up to 0.5 mm could be achieved for molten hot glue and 3% of the tank volume, independent of the shape or aggregate state of the medium.

## Introduction

In the course of the trend toward the intelligent factory as part of the future project of Industry 4.0, manufacturing companies are faced with considerable challenges. Sales markets demand greater flexibility, products must be customizable and of ever higher quality, and at the same time products and their manufacturing processes are becoming more complex.

In order to achieve a consistently high production quality even with small consumption quantities in dynamic processes, all relevant control variables of an automated manufacturing process must be permanently available. These include the filling quantities of liquids, viscous substances, and free-flowing bulk materials in an increasing number of small and application-specific geometrically adapted storage and process containers, which must be continuously recorded by sensors.

These level of measurements are realized with a wide variety of measuring methods, all of which have their advantages and disadvantages [1–3].

Contact-based measurements, such as guided wave radars [4–6] or capacitive probes [7, 8], have a significant disadvantage that debris can settle, as seen in Fig. 1, which significantly affects the accuracy and dynamic response to fast fill level changes. In addition, these sensors are subjected to a great deal of material stress on and in the probe, if, e.g., the medium or environment temperature is very high.

In [4], we have already investigated contact-based measurements using a guided wave radar. However, for the reasons mentioned above, these are not suitable for every application.

In this paper, the accuracy of fill level measurement of low-permittivity material in small metallic tanks is analyzed using an M-sequence ultra wideband (UWB) radar. An earlier version of this paper presents our first results in this direction and was published in the *Proceedings of the EuCAP2022 Conference* [9].

The great advantage of UWB radars is the possibility of noncontact measurements, even under difficult conditions, such as high temperature differences, where, e.g., ultrasonic probes would have a reduced accuracy [10]. But contactless radar measurements also have a main disadvantage. Due to the propagation of electromagnetic waves in free space, a number of multipath reflections are generated, which can negatively affect the measurement. To reduce this effect, electrically large [11, 12] or lense antennas [13] are often used to focus the beam of the electromagnetic waves. However, this is only possible to a limited extent in small containers, since the installation space does not allow for large antennas.

© The Author(s), 2023. Published by Cambridge University Press in association with the European Microwave Association. This is an Open Access article, distributed under the terms of the Creative Commons Attribution licence (<http://creativecommons.org/licenses/by/4.0>), which permits unrestricted re-use, distribution and reproduction, provided the original article is properly cited.

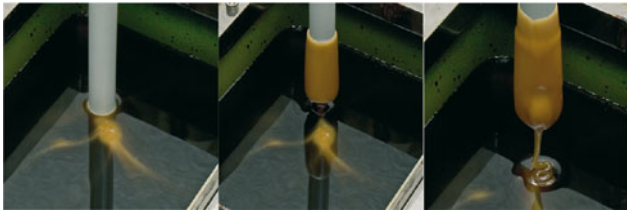


**Figure 1.** A capacitive-level probe located in a hot melt container and is being pulled out slowly (from left to right).

In the future, it is planned to be able to analyze the material properties of the filling material more closely by contactless measurement. For the analysis of stratifications, e.g., it is important to be able to look inside the material. The penetration depth of the electromagnetic wave is directly dependent on the frequency. The lower the frequency, the deeper the electromagnetic wave can penetrate into the filling material. However, common radar-level sensors use a very high center frequency [14–16]. For this reason, this paper investigates the feasibility and achievable accuracy of radar measurements with low frequencies and an electrically small patch antenna under the influence of large multipath components as a basis for further investigations.

First, the principle of level measurement using radar is explained and the experimental setup is described. Afterward, measurement results of hot melt are shown and discussed as an exemplary application. Overall, two methods are considered. The first method is used for level measurement over the complete container height based on a time of flight or distance measurement of the transmit signal. By means of the presented method, a lower accuracy is to be expected, especially close to the empty level, as interference effects between the ground reflection and the reflection of the filling material surface occur here in particular. Thereby, the distance measurement is distorted due to deformations of the transmitted signal caused by this interference. However, high accuracy is required for industrial applications, e.g., hot glue, where the container can be overheated when the container is completely emptied. For this reason, an additional method is shown that specifically considers the empty state.

### Formulation of the problem

The basic principle of the UWB radar level measurement is based on a time-of-flight or distance measurement. When the wave emitted by the radar hits a medium such as water or hot melt, part of it is reflected and another part penetrates the medium. The amount of the reflected part depends on the permittivity of the medium and the frequency. The reflected signal is received again and the level can be inferred by measuring the time of flight. This principle is shown in Fig. 2. On the left, there is the resulting signal with the reflection of the antenna connection due to imperfect matching, the reflection of the hot melt surface, the reflection of the bottom as well as some multiple reflections. The width of the pulse is directly dependent on the bandwidth of the signal. The wider the bandwidth of the signal, the narrower the pulse. Thus, with wider bandwidth, different reflections, such as the ground reflection and the multipath components, can be resolved. For this reason, it is advantageous to use a radar with a large bandwidth for level measurement.

It is easy to see that the reflection of the hot melt surface has a very low amplitude or signal-to-noise ratio (SNR). In addition,

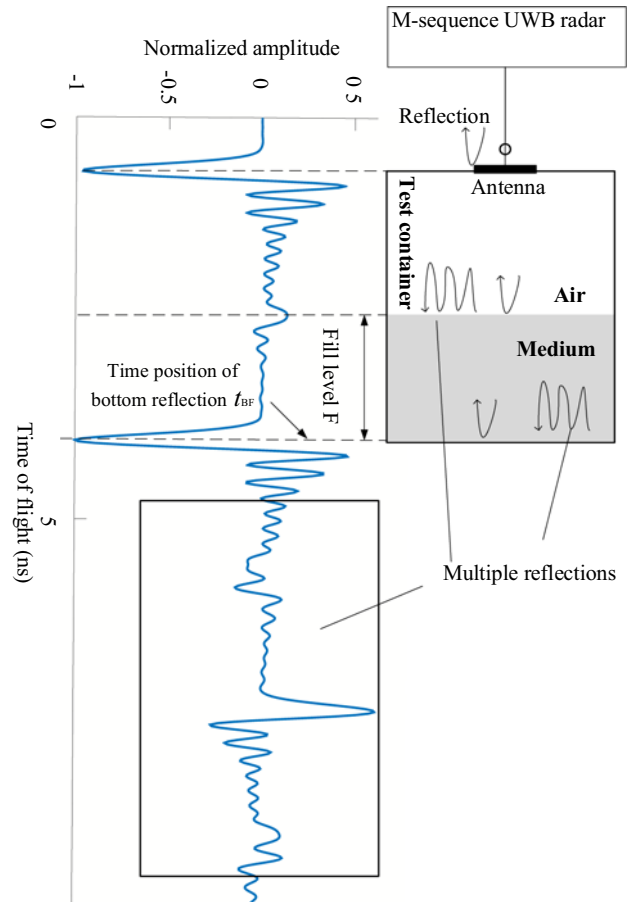


**Figure 2.** Resulting signal reflections of an UWB radar inside a tank without side wall reflections and illustration of the principle of level measurement.

the static reflection of the antenna feeding point and the level-dependent bottom reflection are dominant and would strongly influence the reflection by interference if the filling material surface comes close to these reflections. For this reason, a determination of the temporal position of the bottom reflection is more suitable in order to calculate the level, analyzing the signal component that has been transmitted in the filling medium and reflected from the bottom.

This so-called transmission measurement is usually used to determine the electromagnetic properties, e.g., the permittivity, of a medium [17]. Thereby, the level or thickness of the medium to be investigated is known. We assume that the permittivity is known and the level or thickness is unknown. Thus, the transmission measurement can be adapted to determine the level.

Electromagnetic waves have a lower propagation speed in the medium than in the air. Accordingly, the temporal position of the reflection  $t_{BF}$  changes as a function of the level.

$$t_{BF} = \underbrace{t_{B0} - \frac{2F}{c_0}}_{\text{air}} + \underbrace{\frac{2F}{c_0} \sqrt{\varepsilon_1}}_{\text{filling material}}, \quad (1)$$

where  $t_{BF}$  is the temporal position of the bottom reflection at the fill level  $F$ ,  $t_{B0}$  is the bottom reflection of the empty tank,  $c_0$  is the propagation speed in the air, and  $\varepsilon_1$  is the permittivity of the medium filled in the tank.

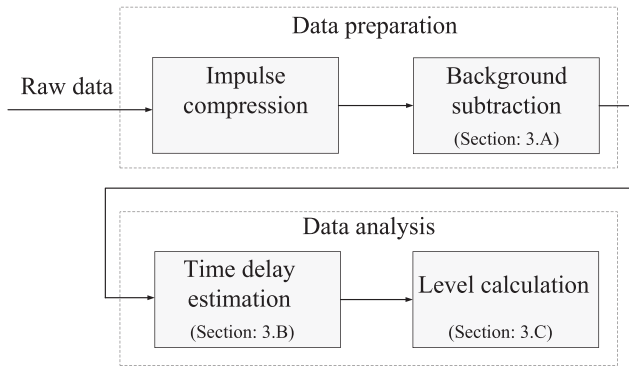


Figure 3. Signal processing chain represented as a flow graph.

With the relation in (1) and the known permittivity of the material, the level can be determined as follows:

$$F(t_{BF}) = \frac{t_{BF} - t_{BO}}{2(\sqrt{\epsilon_1} - 1)} c_0. \tag{2}$$

It should be noted that this formula must be considered carefully for  $\epsilon_1$  very close to 1, since in this case, the smallest errors of the permittivity value would cause large measurement deviations.

### Method of signal processing

In the last section, it was described that the level measurement is based on a radar time-of-flight or distance measurement. In this section, the individual steps of the signal processing are briefly described and discussed. An overview of the different steps from the raw sensor data to the level calculation is shown in Fig. 3.

In time-of-flight measurement, the temporal position of a received pulse or impulse response (IR) is determined. There are different ways to generate the receiving pulse to be analyzed, e.g., by sending a pulse directly or by sending a continuous signal and appropriate post-processing of the receiving signal to get a pulse to be evaluated. All possibilities have their advantages and disadvantages [18, Chap. 4.7]. A detailed consideration of these advantages and disadvantages is beyond the scope of this paper. For the actual signal processing described in this paper, it is not relevant how the temporal pulse was generated for the analysis.

Here, an UWB radar sensor is used, which uses a binary pseudo-random M-sequence generated by a shift register as the transmitted signal. This has several advantages over impulse signals, such as a low crest factor and less influence of jitter. To obtain the raw IR of the scenario for further analysis, a broadband correlation is performed between the transmit and receive signals [18, Chap. 4.7].

### Background subtraction

To subtract static and slowly changing background components, e.g., due to temperature drift effects, the background must be continuously recalculated. A real-time capable background subtraction (BS) method is given by an exponential averaging [21]. We estimate the background  $\bar{h}$  for each observation time indexed by  $k$  with

$$\bar{h}_k(t) = (1 - \beta \cdot \alpha) \bar{h}_{k-1}(t) + \beta \cdot \alpha \cdot h_k(t), \tag{3}$$

where  $\bar{h}_k$  and  $\bar{h}_{k-1}$  are the estimated backgrounds for time indices  $k$  and  $k - 1$ ,  $h_k$  is the IR,  $\alpha \in [0, 1]$  is a scalar weighting factor, and  $\beta$

is a binary value that is based on the calculated difference between two consecutive IRs. The optimal value for  $\alpha$  was experimentally determined to be  $\alpha = 0.99$  for the analyzed measurements. As initial background, we use the measurement of the empty container, where the reflection of the bottom and subsequent multiple reflections are set to zero. Therefore, these reflections are not part of the initial background. The resulting signal  $\hat{h}_k$  is now

$$\hat{h}_k(t) = h_k(t) - \bar{h}_k(t). \tag{4}$$

A special case arises if the fill level does almost not change a moment. In this case,  $\bar{h}_k$  approaches  $h_k$  with (3) and  $\hat{h}_k$  only consists of noise if  $\beta$  is not introduced. Therefore, we set  $\beta$  according to the calculated intensity of level change  $\gamma_k$  inspired by [22]

$$\gamma_k = \sum_{t=0}^T |h_k(t) - h_{k-1}(t)|. \tag{5}$$

We set  $\beta_k = 1$  if  $\gamma_k$  is above a certain threshold and  $\beta_k = 0$  otherwise. In the latter case, no update of the background is performed. To minimize the influence of the slow occurring temperature drift, the current temperature at the antenna is compared in parallel with the temperature at the time of the last update of the BS, if  $\beta_k = 0$ . If the temperature difference near the feeding point exceeds 1 K,  $\beta_k = 1$  is set for one measurement to be able to compensate for very slow temperature drift effects even at long-lasting levels.

### Delay time estimation

A physically realizable signal always has a temporal extension and can also consist of several maxima, as can be seen in Fig. 2. Accordingly, several definitions exist for the time position of an impulse, e.g., by exceeding a threshold value, a local maximum of the impulse, or the energetic center [19]. We have used the time position of a selected local pulse maximum. UWB radars can determine distance changes with very high precision by tracking a selected maximum over the observation time. In principle, it does not matter which maximum is used for the measurement as long it can be ensured that there is no jumping between two maxima. This could lead to an error of several centimeter. For this reason, it is best to choose the maximum according to a criterion that is as unique as possible. The measured absolute temporal position of the pulse depends on the choice of the maximum and the method for determining the maximum. For this reason, it is also clear that a calibration measurement is necessary for an exact assignment of pulse maximum and level. In our case, this is the measurement of the empty tank, since we also want to use the bottom reflection for level determination.

Without further signal processing, the accuracy of the level measurement is limited by half the sampling interval of an IR. In this case, this would be approximately 1.1 cm. If better accuracy is desired, further signal processing steps are necessary, which increase the computational complexity. A trade-off must be found at this point. Radar sensors can be expected to achieve an accuracy in the millimeter range over the entire height of the container. For this reason, the resolution of the signal processing should also be at least in the millimeter range. However, a resolution in the micrometer range is advantageous in order to detect even small level changes quickly and thus make the system more dynamic.

In order to achieve an accuracy of the delay estimation below the sampling interval  $\Delta t$ , the data usually is interpolated first. The fast Fourier transform (FFT) method using zero padding in the frequency domain is suitable for this.

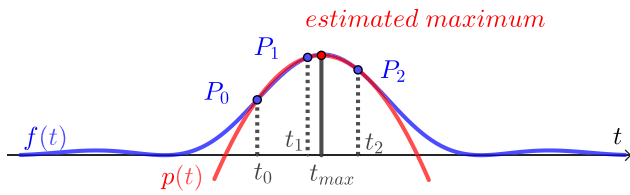


Figure 4. Maximum estimation of a function  $f$ , comp. [20]

Using the zero padding approach, however, still ties the resolution to a grid. Applying additional methods promises subsample estimation, so that higher accuracy can be met with little further processing complexity. One such algorithm is introduced in [20], where it is used to estimate the exact sinusoid frequency of a signal. The therein proposed method for estimation of a local maximum is not limited to the frequency realm and can be applied in two steps to any discrete signal with the objective of finding a local maximum independent of the discrete grid. The intention of the first step is to ensure the points are not located on a side lobe of the signal before introducing them into the second step. Since the sample grid of the UWB radar is known to always be finer than the width of the maximum, this calculation can be omitted completely. In the second step, the exact time delay of the maximum is obtained by fitting a parabola in the chosen set of points as shown in Fig. 4.

The parabola can be described as  $p(t) = At^2 + Bt + C$ , generating the system of equations

$$\begin{pmatrix} t_0^2 & t_0 & 1 \\ t_1^2 & t_1 & 1 \\ t_2^2 & t_2 & 1 \end{pmatrix} \begin{pmatrix} A \\ B \\ C \end{pmatrix} = \begin{pmatrix} P_0 \\ P_1 \\ P_2 \end{pmatrix},$$

where  $P_n$  is the respective amplitude at time sample  $t_n$ . This system can be solved for the parabola coefficients, which in turn can be used to calculate its vertex with  $t_{\max} = -\frac{B}{2A}$ , resulting in

$$t_{\max} = \frac{1}{2} \frac{t_2^2(P_0 - P_1) + t_1^2(P_2 - P_0) + t_0^2(P_1 - P_2)}{t_2(P_0 - P_1) + t_1(P_2 - P_0) + t_0(P_1 - P_2)}.$$

This  $t_{\max}$  is an accurate temporal position estimation of the IR. It should be noted that this algorithm performs better when the closer the chosen points are to each other and the true apex of the signal. Therefore, with regard to the grid spacing in relation to the observed maximum width, an  $r$  interpolation with the factor 5 is performed prior to the parabolic interpolation described above.

A consistently high accuracy of the level measurement over the complete container height has, however, further prerequisites. The signal shape must not change during the observation time and fill level. If the shape of the pulse changes even minimally, the position of the maximum used for estimating the time delay also changes. The consequence is a falsification of the level measurement. Reasons for the signal deformation can be interference with other reflections or even temperature drift. However, in Fig. 2, it is easy to see that there are interfering solid reflections that affect the measurement. Particularly disturbing is the direct reflection of the antenna due to mismatch, which can be assumed to be quasi-static. Static or quasi-static interfering reflections are also called background and can be subtracted, reducing the influence to a minimum.

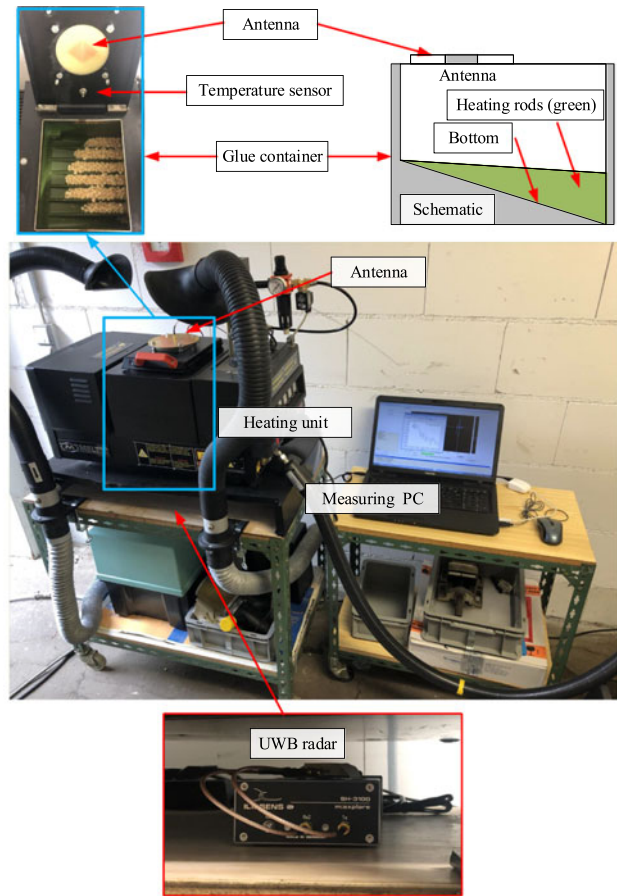


Figure 5. Experimental setup for the evaluation of hot melt level measurements by an M-sequence UWB radar.

### Level calculation

After the time of flight has been estimated, the actual level  $F$  is calculated according to (2). To be able to calculate the level by means of the bottom reflection according to (2), the permittivity of the medium  $\epsilon_1$  and a calibration measurement of the empty vessel are required. If the permittivity of the material  $\epsilon_1$  is not known, it can be determined by, e.g., a transmission measurement [17]. In principle, the same setup can be used as for the actual level measurement if the levels are clearly defined. In this case, the level is known and (1) is converted according to the permittivity.

$$\epsilon_1 = \sqrt{\frac{(t_{BF} - t_{B0})c_0}{2F}} + 1. \tag{6}$$

If this measurement is repeated for different levels, the accuracy of the permittivity measurement (6) can be improved accordingly.

### Measurement setup

The actual measurement setup is shown in Fig. 5. The basic setup is a hot melt dispensing system, which is designed for the precise delivery of a wide variety of hot melt adhesives. Hot melt was chosen as the medium to be investigated, as this is extremely interesting from a scientific and also industrial point of view. Due to the high-temperature differences of over 100 K and relative permittivity close to 1, an accurate measurement of the level is a great challenge.

**Table 1.** Specifications of the UWB radar used

Parameter	Value
10 dB frequency range (radar)	0.1–6 GHz
10 dB frequency range (antenna)	1.2–9 GHz
10 dB frequency range (system)	1.2–6 GHz
Sampling frequency	13.312 GHz
Measurement speed (max.)	130 Hz
Measurement rate (chosen)	10 Hz
Timebase jitter	<20 fs (rms)
Crest factor	2.6
Samples	4095
Ambiguity time	307.6 ns
Ambiguity range (2 way)	46.1 m
Container volume	7 dm <sup>3</sup>

At the bottom of the hot melt container, there are heating rods that heat the melt to 150°C. At the bottom right of the figure, there is a sketched representation of the tank. The heating rods go down inclined and there may be filling material between the rods. In order to show results that are as relevant to practice as possible, a container with a flat bottom is not used. The bevelling of the bottom serves to melt the hot glue more quickly and is common in industrial plants of this type. This makes it difficult to observe an absolute fill level, as there are several definitions of an empty container. Therefore, this paper also discusses one possible definition of an empty tank.

An electrically small diamond-shaped patch antenna is integrated into the lid of the container. It is fed via a 12th order M-sequence radar with a clock frequency of 13.312 GHz featuring 6 GHz bandwidth. It has various advantages compared to pulse signals such as low crest factor and high temporal stability. For better illustration, the variable and fixed system parameters and characteristics of the measurement setup used for the analyzed measurements are shown in Table 1.

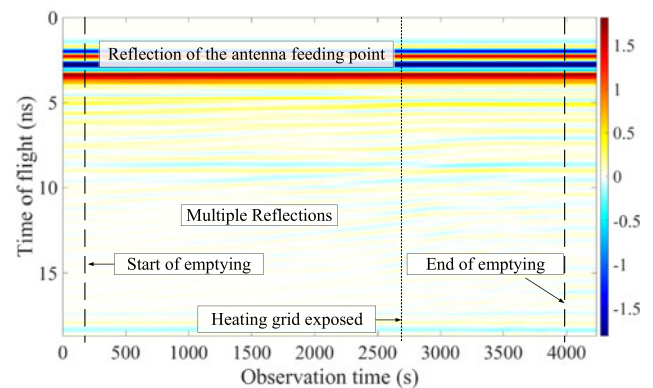
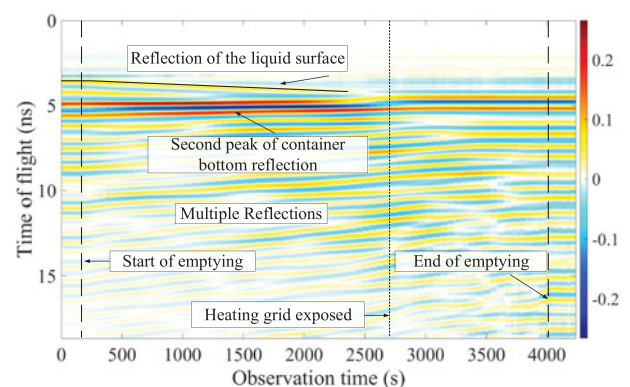
To get the raw IR of the scenario for further analysis, a wideband correlation between transmit and receive signal is performed. A more detailed description of the principle can be found in [23] and [18, Chap. 4.7].

The measurement signal is sent continuously and is periodic. Due to the periodicity of the measurement signal, several measurements can be averaged. This increases the SNR. A prerequisite for an accurate measurement is that the IR must have decayed before the new sequence starts. Since we are in a closed metal container in this application, the decay distance can be many times longer than the container height. For this reason, a high ambiguity range is important.

The temperature is constantly measured at the antenna and at the vessel wall to be able to compensate for drift effects using BS.

## Measurement results

The analysis of the level measurement is divided into two cases in this paper. First, the results of the level measurement are considered over the complete container height and analyzed with regard to accuracy. Since a precise empty state estimation is particularly important for many industrial applications, the next part analyzes

**Figure 6.** Radargram of a container being emptied recorded by an M-sequence UWB radar without background subtraction.**Figure 7.** Radargram of a container being emptied recorded by an M-sequence UWB radar after background subtraction.

what accuracy can be achieved here. The focus is on the detection of whether or not there is material in the container. The actual level measurement plays no role in the second case.

## Measurement data

For the analysis of the hot melt level measurement, several measurements were carried out. As an example, the measurement data of an emptying tank is shown in Fig. 6. For reasons of better visualization, only a section of the measurement data is shown. The actual length  $T$  of the IRs is about 300 ns.

The reflection of the antenna feeding point is so strong that dynamic effects are hardly identifiable. This also makes level measurement difficult. For this reason, a BS according to (4) is performed. The result is shown in Fig. 7. For a better overview, the selected parameters of the signal processing chain for the analysis of the measurements are listed in Table 2.

Two peaks from the reflection of the container bottom are clearly visible, whereas the reflection of the hot melt surface is barely noticeable. As soon as the heating rods are only minimally exposed, any change in the radargram is hardly noticeable. In addition, a large number of multiple reflections can be seen.

The reflection caused by the bottom has a different slope because the propagation speed in the medium is lower than in the air. A closer look at the ground reflection shows that it is insignificantly influenced by the multipath components, as these

**Table 2.** Parameter of the signal processing described in the Section “Formulation of the problem” and Part “Delay Time Estimation”

Parameter	Value
$\alpha$	0.99
$\gamma$	0.009
Interpolation factor	5

only appear after the ground reflection. For this reason, the level measurement accuracy is not expected to be influenced by the multipath components.

The measurement data show that BS is indispensable; otherwise, static reflections, such as those of the feeding point, would significantly worsen the accuracy of the measurement.

### Fill level measurement

Section “Formulation of the problem” Part “Delay Time Estimation” establishes that a constant pulse shape is crucial to achieve high accuracy in level measurement. Any deformation of the pulse, e.g., due to interference, would affect the accuracy of the measurement. In Fig. 7, it can be seen that the reflections of the hot melt surface and that of the bottom interfere with each other at low fill levels. The second local peak of the bottom is visibly less affected by this interference than the first local peak of the bottom reflection.

In general, it does not matter which local peak is selected for the fill level measurement since a calibration measurement is always required to determine the absolute fill level. For this reason, the second local peak of the bottom reflection can be used for the calculation of the fill level. In the measurement, this selection is realized by taking the second local peak, which has a threshold value of 60% of the global pulse maximum of the corresponding IR. This criterion was stable across all measurements. Furthermore, it was apparent that the influence due to the high number of multipath components could be neglected, as these always appear after the ground reflection. Thus, they do not influence the selected peak. By means of the selected threshold as a unique selection criterion, jumping between different local maxima could be prevented and further tracking was not necessary.

To be able to calculate the level by means of the bottom reflection according to (2), the permittivity of the medium and a calibration measurement of the empty vessel are required. The permittivity was measured by a transmission measurement in a well-defined container with a flat metal bottom and calculated according to (6). To increase the accuracy of the measurement, several levels were measured as a function of temperature. The average permittivity over the complete covered frequency range up to 6 GHz is 1.7 at 25°C and 2.5 at 150°C. The temperature dependence is nearly linear.

For the purposes of the investigations in this paper, it is assumed that the hot melt has an approximately homogeneous temperature of 150°C. This assumption was confirmed by holding a temperature probe in the liquid at various points and depths. A prerequisite for this assumption is that the hot melt is completely liquefied. Further investigations with different temperature profiles are currently being carried out.

The fact that the bottom consists of heating rods inclined downwards raises the question of how to define the empty or zero fill level. This is defined as the moment when the heating rods are minimally exposed, as this is a very critical case for industrial

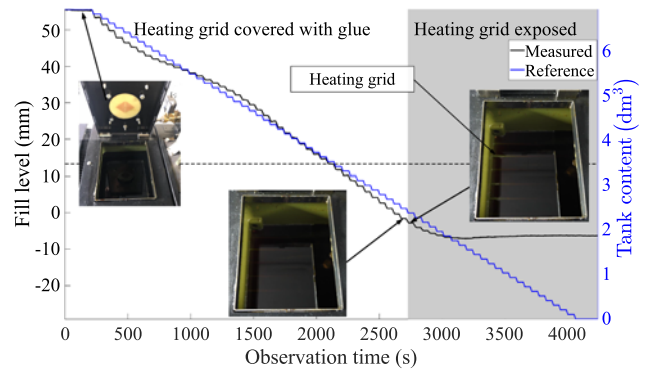


**Figure 8.** Results of the fill level measurement of an emptying hot melt container.

applications. A completely empty tank was used for the calibration measurement, as this condition was the most defined to achieve.

To rate the accuracy of the fill level determination, a reference measurement was conducted. The vessel was emptied stepwise by a fixed volume fraction, resulting in a uniform level change of 2 mm until the heating rods are exposed. In Fig. 8, the reference measurement and results of the fill level measurement are shown. It can be seen that the container was emptied in 2 mm increments, and each fill level was kept for a short time. In addition, the measured fill level does not follow a straight line as expected.

This may be due to strong interference or asymmetric geometry of the tank. Once the heating rods are only minimally exposed, a level change is hardly noticeable. In addition, the zero level is indicated 2.5 mm before the heating rods are exposed. However, despite the fact that the investigated hot melt has such low backscatter properties that the level is calculated indirectly via the bottom reflection, an accuracy of better than 5% of the container height, limited to an absolute accuracy of better than 3 mm, could be achieved.

The accuracy refers to the complete container height. It is also interesting to see the precision with which a level change can be detected. Thus, how much must a specific level change in order for this change to be detected? To rate the precision of the level change detection, a reference measurement was conducted. The level was held at a total of 30 different levels. Then the container was emptied stepwise by a fixed volume fraction, resulting in a uniform level change of 0.1 mm. A more precise analysis is not possible with the measurement setup. For a more precise analysis, a correspondingly precise reference system must be installed, which was not available. Using the fitting method described in the section “Method of signal processing” Part “Delay Time Estimation”, a precision of 0.1 mm in the detection of level changes could be achieved. The fitting method described is a variant for high-resolution time-of-flight estimation. Other methods can be expected to achieve similar or even better resolutions. The trade-off between achievable accuracy and computational complexity always plays a role. There is no perfect choice but always depends on the intended application.

### Empty limit state

Depending on the application, the accuracy of the level measurement mentioned above may not be sufficient, especially for limit levels. Hot melt containers, for example, are not allowed to run empty at any time; otherwise, they could overheat or the suction pump would draw air. Both can severely damage the unit.

For this reason, an empty state measurement or warning should be as precise as possible.

What is a big disturbing factor in the exact determination of the filling level is of utmost advantage in the determination of the empty state. The reflection of the metal is so characteristic that a minimal exposure of the container bottom will greatly change the IR of the system. This effect is used here.

As mentioned above, an empty state calibration is made for the level calculation. For the estimation of the empty limit state, the IR of this calibration measurement  $\bar{h}_E(t)$  is stored and subtracted from the currently measured IR  $h_k(t)$  and the mean squared deviation  $MSD_k$  compared to the empty state is calculated

$$MSD_k = \frac{1}{T} \sum_{t=0}^T (h_k(t) - \bar{h}_E(t))^2 \quad (7)$$

The investigations have shown that the IR of the empty tank is only slightly dependent on the temperature. Thus, it was possible to define a temperature-independent threshold  $MSD_{\text{thresh}} = 0.3$  for  $MSD_k$ , below which the container is assumed to be empty.

Hot glue can occur in several states in the container. These are shown in Fig. 9. In operation, the adhesive is often liquid like in Fig. 9(a). However, it is also possible that the container is filled with granules. This can be seen in Fig. 9(c) and 9(d). When filled with hot melt granules, a bulk cone is usually formed. The position of the cone determines how large the minimum quantity of granules must be in order to be detected by the radar. For this reason, several cone positions were investigated. Furthermore, it is also common in industrial plants to use blocks such as the one shown in Fig. 9(b) from other hot-melt adhesives that have been heated up but not used. This is done in particular to save material and should therefore also be investigated.

**Melted hot melt.**

The results for the melted hot melt are exemplified in Fig. 10. At higher fill levels,  $MSD_k$  is large and approximately independent of the fill level. As the fill level approaches the bottom, a proportionality between the fill level and  $MSD_k$  can be seen.

As soon as the heating rods at the bottom are only slightly exposed, the change in  $MSD_k$  is only slight. The steadily decreasing course of the deviation after the release of the heating rods at the bottom is due to the fact that the completely empty container was taken as a reference.

**Granules.**

In many applications, there are bulk materials in the container. Thus, the delivered form of hot melt for industrial plants is usually also granules.

The analysis results of the granules are shown exemplarily in Fig. 11. Depending on the position of the bulk cone, the granules are only reliably detected from a minimum quantity. In all positions of the cones, stable detection of the granules was observed as soon as a heating rod was partially covered. In this case, as soon as a volume of 0.2 dm<sup>3</sup> was filled in. This corresponds to approximately 3% of the container volume. Similar accuracy was found with other containers up to a volume of 69 dm<sup>3</sup>. Larger containers have not yet been investigated.

**Blocks.**

Next, we consider the detection of glue blocks, which are so common in industrial plants. These glue blocks occur, for example,

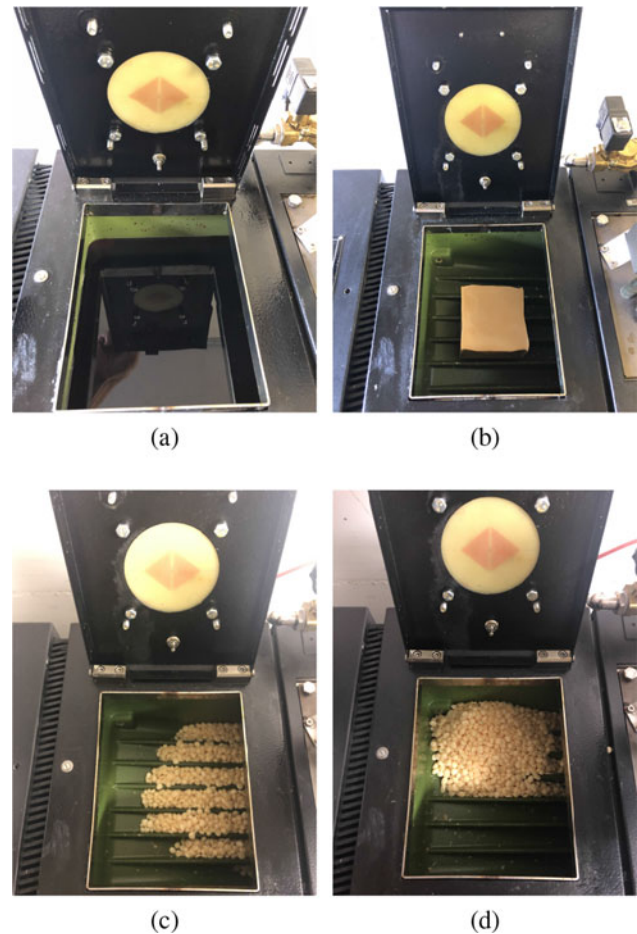


Figure 9. Investigated states of the hot glue for the empty state estimation.

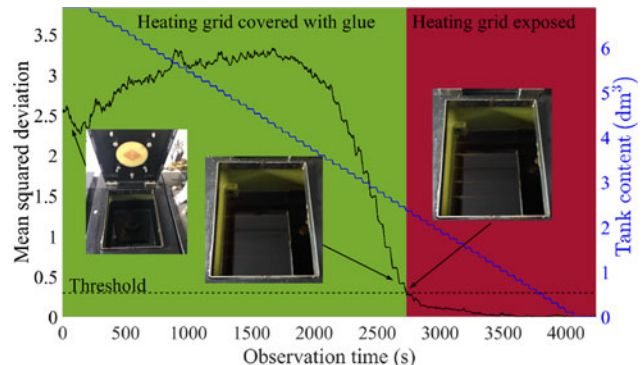
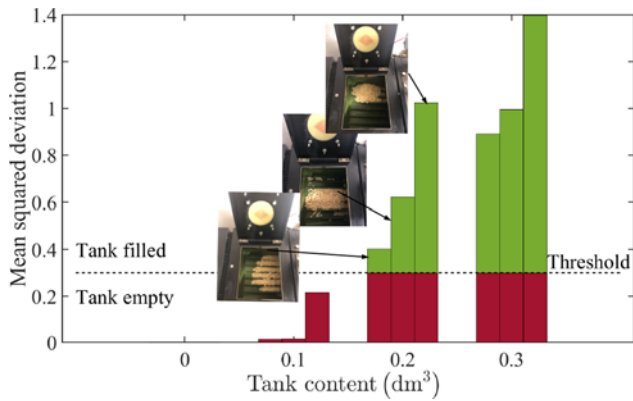
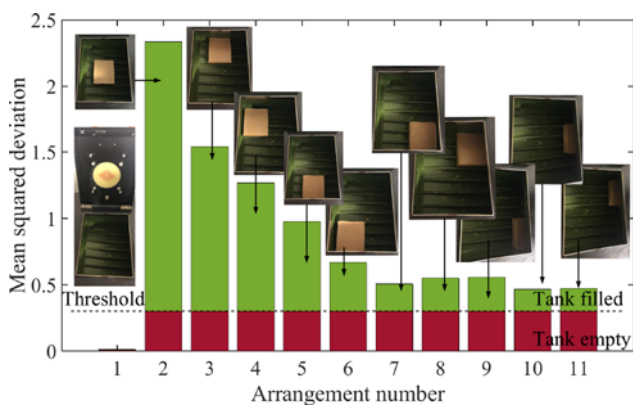


Figure 10. Results of the empty state estimation of an emptying hot melt container.

when the plant has to be completely emptied for cleaning. However, the adhesive is to be reused. One block has a volume of 0.2 dm<sup>3</sup>. As expected, the  $MSD_k$  depends strongly on the position of the block. For this reason, a block was placed at several positions. The results of the analysis can be seen in Fig. 12. Already one block is detectable independent of position. This analysis was also performed for container sizes up to 69 dm<sup>3</sup>. Here, too, an achievable minimum filling quantity of 3% of the container volume was found.



**Figure 11.** Results of detection of adhesive granules at different bulk cone positions in the investigated container.



**Figure 12.** Results of detection of a block of solid adhesive at different positions in the investigated container.

### Summarized.

The measurement was repeated several times over the course of half a year to test the long-term stability of the system. An accuracy of up to 0.5 mm for melted hot melt and 3% of the tank volume independent of the form or aggregate state of the medium could be achieved for the empty state indication, whereby the threshold value was not changed. The calibration measurement of the first measurement run was used for the analysis. Thus, it could be shown that the calibration is also long-term stable. This is particularly interesting for practical applications.

### Conclusion and outlook

This paper presented a novel method of using an M-sequence UWB radar to determine the level of materials with extremely low permittivity. The main idea is to infer the level by measuring the time the electromagnetic wave needs to be reflected by the container bottom given a different wave velocity in the fill medium. An accuracy of better than 5% of the complete container height, limited to an absolute accuracy of better than 3 mm, could be achieved. No significant disturbing influence of multipath components was observed. Furthermore, an independent possibility of precise long-term stable empty state estimation was shown, since especially the empty state is very critical for many industrial applications and therefore should be determined especially precisely. The only requirement for this estimation is an empty

state calibration, which is very easy to perform by measuring the empty container. Therefore it is especially interesting for industrial applications.

In addition to the filling level, the detection of layers is also very important. For example, the hot melt in the container under investigation is heated from below. The pump could therefore already start emptying the container when the lowest layer of glue has melted. However, this layering must be detected by radar. Further investigations in this direction would be of great practical interest. Here, the integration of data fusion [24] or machine learning [25–27] could also be of great relevance.

**Funding Statement.** This work was partly supported by the German Federal Ministry for Economic Affairs and Energy (BMWi) under research contracts ZF4463501RR7 and ZF4087105RR7.

**Competing interest.** The author(s) declare none.

### References

- Hanni JR and Venkata SK (2020) Does the existing liquid level measurement system cater the requirement of future generation?. *Measurement* **156**, 107594.
- Loizou K and Koutroulis E (2016) Water level sensing: State of the art review and performance evaluation of a low-cost measurement system. *Measurement* **89**, 204–214.
- Mohindru P (2023) Development of liquid level measurement technology: A review. *Flow Measurement and Instrumentation* **89**, 102295.
- Wegner TE, Del Galdo G and Gebhardt S (2021) Accuracy of fill level measurement by an M-sequence UWB guided wave radar. *2021 15th European Conference on Antennas and Propagation (EuCAP)*, 1–4. doi: 10.23919/EuCAP51087.2021.9411205
- Kaineder A, Stelzer A, Michenthaler C and Hammerschmidt D (2019) Guided wave tank level sensor. *2019 49th European Microwave Conference (EuMC)*. Paris, France, 936–939. doi: 10.23919/EuMC.2019.8910870
- Cataldo A, Tarricone L, Vallone M, Attivissimo F and Trotta A (2008) Uncertainty estimation in simultaneous measurements of levels and permittivities of liquids using TDR technique. *IEEE Transactions on Instrumentation and Measurement* **57**(3), 454–466.
- Kumar B, Rajita G and Mandal N (2014) A review on capacitive-type sensor for measurement of height of liquid level. *Measurement and Control* **47**(7), 219–224.
- Chetpattananondh K, Tapoanoi T, Phukpattaranont P and Jindapetch N (2014) A self-calibration water level measurement using an interdigital capacitive sensor. *Sensors and Actuators A: Physical* **209**, 175–182.
- Wegner TE, Gebhardt S and Del Galdo G (2022) Level measurement of low-permittivity material using an M-sequence UWB radar. *2022 16th European Conference on Antennas and Propagation (EuCAP)*, 1–5. doi: 10.23919/EuCAP53622.2022.9769405
- Vossiek M, Haberberger N, Krabbe L, Hehn M, Carlowitz C and Stelzig M (2023) A tutorial on the sequential sampling impulse radar concept and selected applications. *IEEE Journal of Microwaves* **3**(1), 523–539.
- Vogt M and Gerding M (2017) Silo and tank vision: Applications, challenges, and technical solutions for radar measurement of liquids and bulk solids in tanks and silos. *IEEE Microwave Magazine* **18**(6), 38–51.
- Heddallikar A, Rathod AH and Pethkar H (2020) Level estimation with radar level probe using multipath reduction technique. *2020 URSI Regional Conference on Radio Science (URSI-RCRS)*, 1–4. doi: 10.23919/URSIRCRS49211.2020.9113637
- Vogt M (2018) Radar sensors (24 and 80 GHz range) for level measurement in industrial processes. *2018 IEEE MTT-S International Conference on Microwaves for Intelligent Mobility (ICMIM)*, 1–4. doi: 10.1109/ICMIM.2018.8443505
- Emerson, About non-contacting radar. 14\_Emerson.com. [https://www.14\\_Emerson.com/en-us/automation/measurement-instrumentation/level/continuous-level-measurement/about-non-contacting-radar](https://www.14_Emerson.com/en-us/automation/measurement-instrumentation/level/continuous-level-measurement/about-non-contacting-radar) (accessed 6 April 2023).

15. Radar level measurement. de.15\_Endress.com. [https://www.de.15\\_Endress.com/en/field-instruments-overview/level-measurement/Radar-level-measurement](https://www.de.15_Endress.com/en/field-instruments-overview/level-measurement/Radar-level-measurement) (accessed 6 April 2023).
16. Radar level transmitters. de.16\_Krohne.com. [https://de.16\\_Krohne.com/en/products/level-measurement/level-transmitters/radar-fmcw-level-transmitters](https://de.16_Krohne.com/en/products/level-measurement/level-transmitters/radar-fmcw-level-transmitters) (accessed 6 April 2023).
17. **Li L, Tan AE-C, Jhamb K and Rambabu K** (2012) Buried object characterization using ultra-wideband ground penetrating radar. *IEEE Transactions on Microwave Theory and Techniques* **60**(8), 2654–2664.
18. **Sachs J** (2012) *Handbook of Ultra-Wideband Short-Range Sensing: Theory Sensors Applications*, Weinheim: John Wiley & Sons.
19. **Sachs J** (2014) On the range estimation by UWB-radar. *2014 IEEE International Conference on Ultra-WideBand (ICUWB)*, Paris, 119–124. doi: 10.1109/ICUWB.2014.6958962
20. **Djukanović S** (2017) Sinusoid frequency estimator with parabolic interpolation of periodogram peak. *2017 40th International Conference on Telecommunications and Signal Processing (TSP)*, 470–473. doi: 10.1109/TSP.2017.8076030
21. **Zetik R, Crabbe S, Krajinak J, Peyerl P, Sachs J and Thomä RS** (2006) Detection and localization of persons behind obstacles using M-sequence through-the-wall radar. *Proceedings of SPIE—The International Society for Optical Engineering*. doi: 10.1117/12.667989
22. **Lee JM, Choi JW and Cho SH** (2016) Movement analysis during sleep using an IR-UWB radar sensor. *2016 IEEE International Conference on Network Infrastructure and Digital Content (IC-NIDC)*, 486–490. doi: 10.1109/ICNIDC.2016.7974622
23. **Sachs J, Peyerl P and Roßberg M** (1999) A new UWB-principle for sensor-array application. *IEEE Instrumentation and Measurement Technology Conference*, Italy, May.
24. **Santhosh KV, Joy B, Rao S and Potirakis SM** (2020) Design of an instrument for liquid level measurement and concentration analysis using multisensor data fusion. *Journal of Sensors* **2020**, 4259509.
25. **Rajalakshmy P, Subha Hency Jose P, Rajasekaran K, Varun R and Sweety Jose P** (2022) *A novel sensing technique for continuous monitoring of volume in an automobile fuel tank*. In M Kathiresh, GR Kanagachidambaresan and SS Williamson (eds), *E-Mobility. EAI/Springer Innovations in Communication and Computing*, Cham: Springer.
26. **Duysak H and Yiğit E** (2019) Level measurement in grain silos with extreme learning machine algorithm. *2019 Scientific Meeting on Electrical-Electronics & Biomedical Engineering and Computer Science (EBBT)*, Istanbul, Turkey, 1–4. doi: 10.1109/EBBT.2019.8742047
27. **Borg D, Serpa Sestito G and da Silva MM** (2021) Machine-learning classification of environmental conditions inside a tank by analyzing radar curves in industrial level measurements. *Flow Measurement and Instrumentation* **79**, 101940.



**Tim Erich Wegner** received the B.Sc. and M.Sc. degrees in electrical engineering and information technology from Technische Universität Ilmenau, Germany, in 2016 and 2018, respectively. He is a researcher at the Electronic Measurement and Signal Processing Group and pursuing the Dr.-Ing. degree. His research interests include signal processing and data fusion for ultra wideband radar applications.



**Stefan Gebhardt** studied industrial and electrical engineering at Technische Universität Ilmenau. In 2014, he received his doctoral degree on the topic of capacitive tomography. He is currently working as a senior development engineer at RECHNER Sensors GmbH, where he is responsible for research activities and developments in the field of level measurement technology.



**Giovanni Del Galdo** studied telecommunications engineering at Politecnico di Milano. In 2007, he received his doctoral degree from Technische Universität Ilmenau on the topic of MIMO channel modeling for mobile communications. He then joined Fraunhofer Institute for Integrated Circuits IIS working on audio watermarking and parametric representations of spatial sound. Since 2012, he leads a joint research group composed of a department at Fraunhofer IIS and, as a full professor, a chair at TU Ilmenau on the research area of electronic measurements and signal processing. His current research interests include the analysis, modeling, and manipulation of multidimensional signals, over-the-air testing for terrestrial and satellite communication systems, and sparsity promoting reconstruction methods.